Scattering of an elastic wave by a single dislocation

Agnès Maurel[a)]
Laboratoire Ondes et Acoustique, UMR CNRS 7587, Ecole Supérieure de Physique et de Chimie Industrielles, 10 rue Vauquelin, 75005 Paris, France

Jean-François Mercier
Laboratoire de Simulation et de Modélisation des Phénomènes de Propagation, URA 853, Ecole Nationale Supérieure des Techniques Avancées 32 bd Victor, 75015 Paris, France

Fernando Lund
Departamento de Física, Facultad de Ciencias Físicas y Matemáticas, Universidad de Chile, Casilla 487-3, Santiago, Chile and Centro para la Investigación Interdisciplinaria Avanzada en Ciencias de los Materiales (CIMAT), Santiago, Chile

(Received 29 June 2003; revised 18 January 2004; accepted 26 January 2004)

The scattering amplitude for the scattering of anti-plane shear waves by screw dislocations, and of in-plane shear and acoustic waves by edge dislocations are computed within the framework of elasticity theory. The former case reproduces well-known results obtained on the basis of an electromagnetic analogy. The latter case involves four scattering amplitudes in order to fully take into account mode conversion, and an adequately generalized optical theorem for vector waves is provided. In contrast to what happens for scattering by obstacles, the scattering amplitude increases with wavelength, and, in general, mode conversion in the forward direction does not vanish.
 [DOI: 10.1121/1.1687735]

PACS numbers: 43.20.GP, 43.35.Cg, 43.40.Fz [ANN] Pages: 2773–2780

I. INTRODUCTION

The interaction of an elastic wave with inclusion-like defects has received quite a bit of attention, starting with work in the 1950s concerning the scattering of acoustical waves by spherical obstacles that may be empty, fluid filled, or elastic, embedded in an elastic medium.[1–3] Further works consider the case of transverse incident wave both for two-dimensional cylindrical cavities[4,5] and for three-dimensional spherical cavities[6–8] as well as for more complicated inclusion shapes.[9–12]

In addition to inclusions and flaws, which are static obstacles to elastic wave propagation in a solid, and whose interaction provide the underpinning for nondestructive testing,[13–17] dislocations are also defects that interact with acoustic waves. Edge dislocations were introduced as defects in a crystal by Orowan, Polanyi, and Taylor,[18–20] and screw dislocations were introduced by Burgers.[21] Although they play a central role in the understanding of plasticity, it is very difficult to quantitatively measure their properties, a standard tool being electron microscopy. Would it be possible to develop acoustical diagnostic techniques to make quantitative dislocation measurements? A first step in that direction would involve a full understanding of the interaction between elastic waves and dislocations, about which surprisingly little can be found in the literature.

Again in the 1950s, the interaction of elastic waves with dislocations was studied by Nabarro,[22] who noted that waves would be scattered by a dislocation because the motion induced by the incoming wave would generate the emission of a scattered wave. Thus, a description of this mechanism involves two steps: the motion of a dislocation in the presence of an incident wave has to be known as well as a representation for the elastic field generated by a moving dislocation. Eshelby[23,24] and Nabarro[22] used an electromagnetic analogy to tackle the case of a two-dimensional screw dislocation, which reduces to a scalar problem when the interaction is with an anti-plane shear wave. However, this analogy is no longer valid for edge dislocations when both in-plane shear and compressional waves are involved, each one with its own propagation velocity. In 1963, Mura[25] derived from the Navier equations an integral representation for the elastic field generated by a dislocation loop in three dimensions in arbitrary motion, of which two-dimensional cases can be obtained as special cases. Kiusalaas[26] considered the special case of an edge dislocation oscillating with an arbitrary velocity. Also, the expression of the total scattering cross section of an elastic shear wave incident at right angles with the Burgers vector of the dislocation can be found in the conclusion of this paper, suggesting that the authors have used some equation of motion for the edge dislocation. Unfortunately, no calculations are given, the authors indicating that they are too lengthy to be reproduced.

The derivation from the Navier equation of the equation of motion for a dislocation in the presence of an external, time-dependent, stress field has been obtained by Lund.[27] This work, together with the integral representation of Mura,[25] allows for a full description of the scattering of elastic waves by dislocations. This paper carries out this program for both screw and edge dislocations in two dimensions. In the former case, the problem reduces to a scalar problem for the anti-plane (shear) wave. The results obtained are in agreement with those obtained in Ref. 22 using the electromagnetic analogy. The latter case leads to a vector problem

[a)]Electronic mail: agnes.maurel@espci.fr

for the two in-plane (shear and compressional) waves. Thus, accounting for mode conversions, four scattering functions are determined.

In three dimensions, the interaction of sound waves with dislocation segments has been described by the vibrating string model[28–31] based on the formulation of Koehler[32] in which the dislocation is modeled as a scalar string driven by a scalar time dependent stress. This model is very simple, a fact that allows for many applications, and it certainly captures the essence of the physics of the elastic wave–dislocation interaction. It has been quite successful in explaining a wealth of data in acoustics and thermal conductivity experiments.[33] However, it does not consider the many complexities of this interaction. For example, it does not differentiate between edge and screw dislocations, or among the various polarizations available to an elastic wave. The present work presents a full vector treatment of the elastic wave–dislocation interaction in two dimensions.

The paper is organized as follows. Section II presents briefly the integral representation of the scattered wave due to the motion of the dislocation and the equation of motion for a dislocation in the presence of an incident wave. Simplified expressions for the bidimensional problem and in the case of small amplitude and small velocity (well below the speed of sound) motion of the dislocation are given. Sections III and IV treat, respectively, the anti-plane and in-plane cases and the derivation of the scattering functions are presented, as well as the resulting cross sections. It is found in both cases that the scattering strength of a dislocation increases when increasing the wavelength of the incident wave. The explanation for this unusual behavior comes from the particular mechanism of the scattering which differs from the mechanism responsible for the scattering by static inhomogeneity such as inclusions and voids, where a vanishing scattering cross section is expected at long wavelengths. As previously noted, the scattering by a dislocation is a consequence of a dynamic interaction with the incident wave and there is no reason to expect similar results here. Rather, the scattering cross section is linked to the equation of motion of the dislocation in the presence of an incoming wave, a motion whose amplitude does increase with the wavelength in the dynamical models of Refs. 24 and 27. A complete description of the interaction of an elastic wave with a dislocation would also consider the interaction with the core of the dislocation. This would need an atomistic description of the dislocation core. However, this effect can be neglected for elastic wavelengths that are long compared to core size, as is the case for externally generated waves even at the highest ultrasonic frequencies available.

II. BASIC EQUATIONS

The mechanism for the scattering of an elastic incident wave by a dislocation is quite simple: The incident wave hits the dislocation, causing it to oscillate in response. The ensuing oscillatory motion will generate outgoing (from the dislocation position) elastic waves.

The goal of this section is to briefly derive the integral representation of the scattered wave due to the motion of a dislocation (2.4) and the equation of motion of a dislocation (2.5). Equation (2.4) comes from Ref. 25 written in two dimensions and under the hypothesis of small amplitude motion. Equation (2.5) comes from Ref. 27 under the same hypothesis.

In Secs. III and IV, these equations will be used when the dislocation motion is induced by an incident wave.

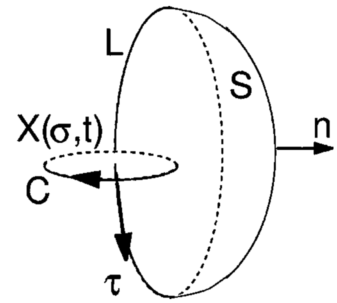

FIG. 1. Definition of the Burgers vector.

A. Scattered wave by a moving dislocation

We consider a dislocation loop $\mathbf{X}(\sigma,t)$, where σ is the coordinate along the loop L in the three-dimensional space with the current coordinates $\mathbf{x}=(x_1,x_2,x_3)$. $\mathbf{b}$ is the Burgers vector, defined by a discontinuity of the displacement field $\mathbf{u}$: $\oint_{\mathcal{C}} d\mathbf{u} \equiv -\mathbf{b}$, formally written $[\mathbf{u}]=\mathbf{b}$, where $\mathcal{C}$ is a closed curve around the dislocation with a direct orientation with respect to $\boldsymbol{\tau}=\partial\mathbf{X}/\partial\sigma$ (Fig. 1).

A homogeneous, linearly elastic solid containing a dislocation loop L is described by displacements $\mathbf{u}(\mathbf{x},t)$ away from an equilibrium position, and the equations of elastodynamics are

$$\rho\frac{\partial^2}{\partial t^2}u_i(\mathbf{x},t)-c_{ijkl}\frac{\partial^2}{\partial x_j\partial x_k}u_l(\mathbf{x},t)=0 \tag{2.1}$$

with boundary conditions

$$[u_i]=b_i,\quad \left[c_{ijkl}\frac{\partial u_l}{\partial x_k}n_j\right]=0 \tag{2.2}$$

across a surface S bounded by the dislocation loop. We consider an isotropic solid, where the elastic constants are $c_{ijkl}=\lambda\delta_{ij}\delta_{kl}+\mu(\delta_{ik}\delta_{jl}+\delta_{il}\delta_{jk})$ with (λ,μ) the Lamé coefficients and ρ is the density. Using the Green function in the three-dimensional free space $G^{0(3D)}$, defined by

$$\rho\frac{\partial^2}{\partial t^2}G^{0(3D)}_{im}(\mathbf{x}-\mathbf{x}',t-t')-c_{ijkl}\frac{\partial^2}{\partial x_j\partial x_k}G^{0(3D)}_{lm}(\mathbf{x}-\mathbf{x}',t-t')$$
$$=\delta(\mathbf{x}-\mathbf{x}')\,\delta(t-t')\,\delta_{im},$$

the displacement u_m generated by a dislocation loop $\mathbf{X}(\sigma,t)$ undergoing arbitrary motion can be written as an integral representation,

$$u_m(\mathbf{x},t)=c_{ijkl}\int\int_{S(t')}dt'\,dS\,b_l n_k\frac{\partial}{\partial x_j}G^{0(3D)}_{im}(\mathbf{x}-\mathbf{x}',t-t'),$$

where $\mathbf{n}$ denotes the normal vector to $S(t)$, the surface of discontinuity for the displacement [$S(t)$ is time dependent since the dislocation line that defines $\mathbf{X}(\sigma,t)$ moves]. Since this surface does not have a special physical significance, it

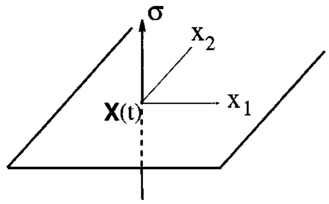

FIG. 2. Configuration of the two-dimensional (2D) problem.

should be possible to express physically meaningful quantities in terms of a source that is localized along the loop L. This was done by Mura[25] taking the time derivative of the preceding expression. Using $\int_{\Delta S} dS\, n_k = \epsilon_{knh} \oint_L d\sigma\, \dot{X}_n \tau_h \Delta t$, where ΔS is an increment of $S(t)$ with respect to a time increment Δt, ϵ_{knh} is the usual completely antisymmetric tensor and an overdot means time derivative. Thus, the velocity $v_m \equiv \dot{u}_m$ is found to satisfy the integral representation:

$$v_m(\mathbf{x},t) = \epsilon_{knh} c_{ijkl} \int \oint_L dt'\, d\sigma\, b_l \dot{X}_n(\sigma,t')\, \tau_h(\sigma) \frac{\partial}{\partial x_j} \times G^{0(3\mathrm{D})}_{im}(\mathbf{x} - \mathbf{X}(\sigma,t'), t-t'). \tag{2.3}$$

In addition to the interest of deriving an integral representation over a curve that has a physical meaning, note that the displacement $\mathbf{u}$ (for which no such integral can be found) is not particularly relevant contrary to its time and space derivatives which appear in expressions of energy and momentum.

We consider now the bidimensional case of a dislocation line along the x_3 axis moving in the plane (x_1, x_2) (Fig. 2). Equation (2.3) takes the form

$$v_m(\mathbf{x},t) = \epsilon_{kn} c_{ijkl} \int dt'\, b_l \dot{X}_n(t') \frac{\partial}{\partial x_j} G^0_{im}(\mathbf{x} - \mathbf{X}(t'), t-t'),$$

where $\epsilon_{ij} \equiv \epsilon_{ij3}$ and $G^0 \equiv \int dx_3\, G^{0(3\mathrm{D})}$ is the Green function in two dimensions. For small amplitude motion of a dislocation near the origin, we have at dominant order $G^0(\mathbf{x} - \mathbf{X}(t'), t-t') \simeq G^0(\mathbf{x}, t-t')$. Since v_m appears as a convolution product, we obtain in the frequency domain

$$v_m(\mathbf{x},\omega) = \epsilon_{kn} c_{ijkl} b_l \dot{X}_n(\omega) \frac{\partial}{\partial x_j} G^0_{im}(\mathbf{x},\omega). \tag{2.4}$$

In order to complete the description of the problem, the motion of the dislocation, $\dot{\mathbf{X}}(t)$, needs to be known.

B. Equation of motion of a dislocation in two dimensions

A method of finding an equation of motion for a dislocation loop can be found in Ref. 27. It is based on the observation that the equations of dynamic elasticity follow from a variational principle, and assumes low accelerations so that the backreaction of the radiation on the dislocation dynamics can be neglected. In two dimensions and under the hypothesis of subsonic bidimensional motion $\dot{X} \ll \alpha$, β, where $\alpha = \sqrt{(\lambda + 2\mu)/\rho}$ and $\beta = \sqrt{\mu/\rho}$ are the shear and compressional velocities, it takes the form:

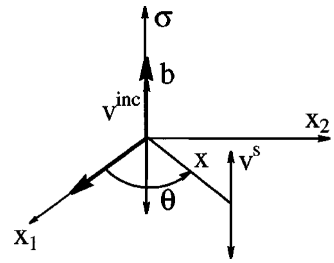

FIG. 3. Shear wave propagating along x_1 (velocity v^{inc}) interacting with a 2D screw dislocation.

$$\frac{\partial}{\partial t}\left(\frac{\partial \mathcal{L}}{\partial \dot{X}_a}\right) = \epsilon_{ab} b_i \Sigma_{ib}, \tag{2.5}$$

where $\Sigma_{ib} = c_{ibkl}(\partial/\partial x_l) u_k$ is the stress tensor [in Eq. (2.5), Σ_{ib} is evaluated at the dislocation position] and $\mathcal{L}$ is the Lagrangian density,

$$\mathcal{L} = -\frac{\mu}{4\pi} \ln\left(\frac{\delta}{\epsilon}\right) \left\{ b_\parallel^2 \left(1 - \frac{\dot{X}^2}{2\beta^2}\right) + b_\perp^2 \left[2(1-\gamma^{-2}) - \frac{\dot{X}^2}{2\beta^2}(1+\gamma^{-4}) \right] + \frac{(b_\perp \wedge \dot{\mathbf{X}})^2}{\beta^2}(1-\gamma^{-4}) \right\},$$

with $\gamma = \alpha/\beta$ and δ, ϵ are the long- and short-distance cut-off lengths, respectively. $b_\parallel$ and $b_\perp$ are the components of the Burgers vector parallel and perpendicular to the dislocation line. Equation (2.5) represents typically an equation for a string endowed with mass forced by the usual Peach–Koehler force.[34] In a more general case, say for oblique wave incidence, there would be additional terms arising from the line tension associated with the dislocation line curvature. A more realistic case would also consider the dislocation's viscosity. Here we neglect this effect for simplicity. Note, however, that even in the absence of an intrinsic dissipation by a single dislocation, the multiple scattering by many dislocations will damp an acoustic wave.[35]

In Secs. III and IV, the response $\dot{\mathbf{X}}(t)$ of screw $(b_\perp = 0)$, and edge $(b_\parallel = 0)$, dislocations to an external elastic wave is derived from Eq. (2.5).

III. THE ANTI-PLANE CASE: SCATTERING BY A SCREW DISLOCATION

Here we consider the two-dimensional problem of the scattering of an elastic wave by a screw dislocation, for which $b_\perp = 0$, interacting with an incident anti-plane shear wave (no interaction with in-plane waves occurs). This is a scalar problem, which is easy to deal with.

A. Derivation of the scattering function

A screw dislocation corresponds to a Burgers vector parallel to the dislocation line $b_i = b\,\delta_{i3}$ (Fig. 3). In the presence of an incident wave $\mathbf{v}^{\mathrm{inc}}$ of frequency Ω, Eq. (2.4) concerns the wave scattered by the dislocation $\mathbf{v}^s = \mathbf{v} - \mathbf{v}^{\mathrm{inc}}$ and simplifies in

$$v^s(\mathbf{x},\omega)=\mu b\epsilon_{ab}\dot{X}_b(\omega)\frac{\partial}{\partial x_a}G^0(\mathbf{x},\omega), \tag{3.1}$$

where v denotes v_3 and $G^0\equiv G^0_{33}$ is the scalar Green function for the shear wave. Since $G^0_{31}=G^0_{32}=0$, the anti-plane case corresponds to the scalar case of the interaction of the anti-plane shear wave with a screw dislocation. As previously said, the integral representation has to be completed with the law for the dislocation motion $\dot{\mathbf{X}}(\omega)$ to be self-consistent. In the case of a screw dislocation, the Lagrangian density reduces to $\mathcal{L}=(\mu b^2/4\pi\beta^2)\ln(\delta/\epsilon)(\dot{X}^2/2-\beta^2)$. Equation of motion (2.5) takes the form

$$M\ddot{X}_b(t)=-\mu b\epsilon_{bc}\frac{\partial u}{\partial x_c}(\mathbf{X}(t),t),$$

with $M=(\mu b^2/4\pi\beta^2)\ln(\delta/\epsilon)$ the usual effective mass per unit length of dislocation.[36,37] For a weak scattering strength, we use the Born approximation ($u=u^{\text{inc}}$ in the term on the right-hand side) and we use the hypothesis of small amplitude motion [$\mathbf{X}(t)$ is taken equal to zero at dominant order for $\Omega X/\beta\ll 1$]. The previous expression takes the following form in the frequency domain:

$$\dot{X}_b(\omega)=-\frac{\mu b}{M\omega^2}\epsilon_{bc}\frac{\partial v^{\text{inc}}}{\partial x_c}(\mathbf{0},\omega). \tag{3.2}$$

The Born approximation is valid for weak interaction, i.e., when the scattered wave is a small correction to the incident wave. That this is a realistic assumption is demonstrated by recent experiments of acoustic waves interacting with dislocations[38–40] where it can be seen that the incident plane wave is only slightly distorted when crossing a dislocation.

Finally, Eqs. (3.1) and (3.2) lead to

$$v^s(\mathbf{x},\omega)=\frac{\mu^2b^2}{M\omega^2}\frac{\partial v^{\text{inc}}}{\partial x_a}(\mathbf{0},\omega)\frac{\partial}{\partial x_a}G^0(\mathbf{x},\omega). \tag{3.3}$$

At the distance x far from the dislocation, the scattering function $f(\theta)$ is defined as the angular dependence of the scattered wave $v^s(\mathbf{x},t)=f(\theta)(e^{i\Omega x/\beta}/\sqrt{x})v^{\text{inc}}(\mathbf{0},t)$ for an incident plane wave $v^{\text{inc}}(\mathbf{x},t)$ of frequency Ω, propagating, say along the x_1 axis, and of unit amplitude $v^{\text{inc}}(\mathbf{x},t)=e^{i\Omega(x_1/\beta-t)}$, with $\theta=(\widehat{Ox_1,\mathbf{x}})$. Using the asymptotic behavior of the Green function $G^0(\mathbf{x},\omega)=(i/4\mu)\dot{H}^{(1)}_0(\omega x/\beta)\simeq(i/4\mu)\sqrt{(2\beta/\pi\omega)}e^{-i\pi/4}(e^{i\omega x/\beta}/\sqrt{x})$, we obtain from Eq. (3.3)

$$v^s(\mathbf{x},t)=\int d\omega\, e^{-i\omega t}\frac{\mu^2b^2}{M\omega^2}\left(\frac{i\Omega}{\beta}\delta(\omega-\Omega)\right)\times\left(-\frac{1}{4\mu}\sqrt{\frac{2\beta}{\pi\omega}}e^{-i\pi/4}\frac{\omega x_1}{\beta x}\frac{e^{i\omega x/\beta}}{\sqrt{x}}\right),$$

from which it is easy to obtain

$$f(\theta)=-\frac{\mu b^2}{2M}\frac{e^{i\pi/4}}{\sqrt{2\pi\Omega\beta^3}}\cos\theta. \tag{3.4}$$

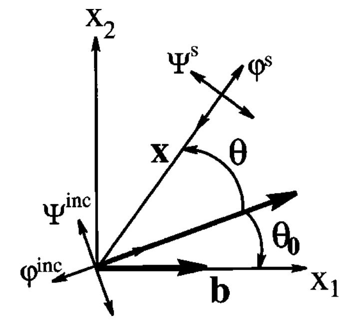

FIG. 4. Acoustic wave (velocity potential φ^{inc}) and in-plane shear-wave (velocity potential ψ^{inc}) interacting with a 2D gliding edge dislocation.

B. Total cross section

The total cross section is classically defined starting from the time averaged total energy flux across a cylinder around the dislocation $\sigma^a=\frac{1}{2}\Re(\int \mathbf{dS}\,\Sigma\,\mathbf{v}^*)$ and decomposing Σ and $\mathbf{v}$ into a sum of the incident part and scattered part. Then, the scattered and total cross sections are defined, with $\sigma^s=-\frac{1}{2}\Re(\int \mathbf{dS}\,\Sigma^s\mathbf{v}^{s*})$ and $\sigma^t=\sigma^a+\sigma^s$. In the scalar case, $\Sigma\mathbf{v}^*$ reduces to $\mu(\partial u/\partial x)v^*$. Normalizing the fluxes with the energy flux $\sigma_0=\mu\Omega^2/2\beta$ of the incident plane wave across a unit surface leads to

$$\frac{d\tilde{\sigma}^s}{d\theta}=|f(\theta)|^2, \tag{3.5}$$

$$\tilde{\sigma}^t=2\Im\left(\sqrt{\frac{2\pi\beta}{\Omega}}f(0)e^{-i\pi/4}\right), \tag{3.6}$$

where $\tilde{\sigma}=\sigma/\sigma_0$. The first relation gives the scattering cross-section $\tilde{\sigma}^s$ and we obtain

$$\tilde{\sigma}^s=\frac{\mu^2b^4}{8M^2\Omega\beta^3}, \tag{3.7}$$

in agreement with Ref. 26. Note that the behavior of the scattering cross section versus frequency Ω, first observed in Refs. 22–24, is unusual since it indicates that the strength of the scatterer increases with wavelength, as opposed to what happens with fixed inclusions. This is discussed further in Sec. V. The second relation is known as the optical theorem.

IV. THE IN-PLANE CASE: SCATTERING OF AN ELASTIC WAVE BY AN EDGE DISLOCATION

We consider in the following the two-dimensional problem of the scattering of an elastic wave by an edge dislocation interacting with incident in-plane compressional and shear waves (Fig. 4). In this case, no interaction with anti-plane wave occurs. The mechanism for such scattering is the same as in the anti-plane case: The dislocation oscillates under the action of the incident wave, producing the emission of scattered waves. The differences come from the vectorial nature of the considered waves: Due to mode conversions, an incident compressional wave produces both compressional and shear scattered waves and the same occurs for an incident shear wave. Thus, in a general case, four scattering functions have to be calculated.

A. Derivation of the scattering functions

The in-plane case corresponds to the interaction of an edge dislocation, for which $b_{\parallel}=0$, with the in-plane waves, propagating at velocities α and β. We restricted ourselves to the case of gliding edge dislocations, for which the line dislocation moves only along its Burgers vector. Dislocation climb is not considered in this paper as it involves diffusive mass transport and cannot be treated within a purely elastic framework.

The velocity of the wave scattered by a gliding edge along the x_1 axis can be expressed using Eq. (2.4), with $b_i=b\,\delta_{i1}$ and $\dot{X}_i=\dot{X}\,\delta_{i1}$,

$$v_m^s(\mathbf{x},\omega)=-b\mu\dot{X}(\omega)\left(\frac{\partial}{\partial x_2}G_{1m}^0(\mathbf{x},\omega)+\frac{\partial}{\partial x_1}G_{2m}^0(\mathbf{x},\omega)\right), \tag{4.1}$$

The motion $\dot{\mathbf{X}}(t)=(\dot{X}(t),0,0)$ of a gliding edge along the x_1 axis submitted to the wave displacement field $\mathbf{u}$ is given by Ref. 27, using Eq. (2.5) with $b_{\parallel}=0$ and $b_{\perp}\wedge\dot{\mathbf{X}}=0$. In this case, the Lagrangian density reduces to $\mathcal{L}=(\mu b^2/4\pi\beta^2)(1+\gamma^{-4})\ln\,(\delta/\epsilon)(\dot{X}^2/2-2\beta^2(1-\gamma^{-2})/(1+\gamma^{-4}))$ and we get

$$M\ddot{X}(t)=\Sigma_{12}b, \tag{4.2}$$

where $M=(\mu b^2/4\pi\beta^2)(1+\gamma^{-4})\ln(\delta/\epsilon)$ is the effective mass per unit length of edge dislocation. As for the case of the screw dislocation, we use the Born approximation to express $\dot{X}(\omega)$ as a function of the incident potentials (for weak scattering). At dominant order, the small parameter being $\Omega X/\alpha,\beta$, we get

$$\dot{X}(\omega)=-\frac{b\mu}{M\omega^2}\left(\frac{\partial v_1^{\mathrm{inc}}}{\partial x_2}(\mathbf{0},\omega)+\frac{\partial v_2^{\mathrm{inc}}}{\partial x_1}(\mathbf{0},\omega)\right), \tag{4.3}$$

so we have

$$v_m^s(\mathbf{x},\omega)=K_m(\mathbf{x},\omega)\frac{b^2\mu^2}{M\omega^2}\left(\frac{\partial v_1^{\mathrm{inc}}}{\partial x_2}(\mathbf{0},\omega)+\frac{\partial v_2^{\mathrm{inc}}}{\partial x_1}(\mathbf{0},\omega)\right), \tag{4.4}$$

with

$$K_m(\mathbf{x},\omega)=\frac{\partial}{\partial x_2}G_{1m}^0(\mathbf{x},\omega)+\frac{\partial}{\partial x_1}G_{2m}^0(\mathbf{x},\omega). \tag{4.5}$$

It now becomes convenient to introduce longitudinal (φ) and shear (ψ) velocity potentials:

$$\mathbf{v}=\boldsymbol{\nabla}\varphi+\boldsymbol{\nabla}\times\boldsymbol{\psi} \tag{4.6}$$

with $\boldsymbol{\psi}=(0,0,\psi)$. The incident wave, propagating in a direction θ_0 with the x_1 axis (Fig. 4), is described by its potentials

$$\begin{aligned}\varphi^{\mathrm{inc}}(\mathbf{x},t)&=A_\alpha e^{i(\Omega/\alpha)(x_1\cos\theta_0-x_2\sin\theta_0)}e^{-i\Omega t},\\ \psi^{\mathrm{inc}}(\mathbf{x},t)&=A_\beta e^{i(\Omega/\beta)(x_1\cos\theta_0-x_2\sin\theta_0)}e^{-i\Omega t}.\end{aligned} \tag{4.7}$$

Far from the dislocation, the scattered potentials are defined by

$$\begin{pmatrix}\varphi^s(\mathbf{x},t)\\ \psi^s(\mathbf{x},t)\end{pmatrix}=\frac{1}{\sqrt{x}}\begin{pmatrix}f_{\alpha\alpha}(\theta)e^{i(\Omega x/\alpha)} & f_{\alpha\beta}(\theta e^{i(\Omega x/\alpha)}\\ f_{\beta\alpha}(\theta)e^{i(\Omega x/\beta)} & f_{\beta\beta}(\theta)e^{i(\Omega x/\beta)}\end{pmatrix}\times\begin{pmatrix}\varphi^{\mathrm{inc}}(\mathbf{0},t)\\ \psi^{\mathrm{inc}}(\mathbf{0},t)\end{pmatrix}, \tag{4.8}$$

where the scattering functions f_{ab}, with $a,b=\alpha,\beta$ denote the a wave resulting from an incident b wave and angle θ is the angle between $\mathbf{x}$ and the direction of propagation of the incident wave (Fig. 4).

To derive the scattering functions, the matrix in Eq. (4.8) has to be found. To do this, we use the following relations:

$$\begin{pmatrix}\varphi^s(\mathbf{x},\omega)\\ \psi^s(\mathbf{x},\omega)\end{pmatrix}=N^s\begin{pmatrix}v_1^s(\mathbf{x},\omega)\\ v_2^s(\mathbf{x},\omega)\end{pmatrix}, \tag{4.9}$$

$$\begin{pmatrix}v_1^s(\mathbf{x},\omega)\\ v_2^s(\mathbf{x},\omega)\end{pmatrix}=N^{s,\mathrm{inc}}(\mathbf{x},\omega)\begin{pmatrix}v_1^{\mathrm{inc}}(\mathbf{x},\omega)\\ v_2^{\mathrm{inc}}(\mathbf{x},\omega)\end{pmatrix}, \tag{4.10}$$

$$\begin{pmatrix}v_1^{\mathrm{inc}}(\mathbf{x},\omega)\\ v_2^{\mathrm{inc}}(\mathbf{x},\omega)\end{pmatrix}=N^{\mathrm{inc}}\begin{pmatrix}\varphi^{\mathrm{inc}}(\mathbf{x},\omega)\\ \psi^{\mathrm{inc}}(\mathbf{x},\omega)\end{pmatrix}, \tag{4.11}$$

where Eqs. (4.9) and (4.11) are simply the relations between velocity and potentials deduced from Eq. (4.6), with

$$N^s=\frac{1}{i\Omega}\begin{pmatrix}\alpha\cos(\theta-\theta_0) & \alpha\sin(\theta-\theta_0)\\ \beta\sin(\theta-\theta_0) & -\beta\cos(\theta-\theta_0)\end{pmatrix} \tag{4.12}$$

and

$$N^{\mathrm{inc}}=i\Omega\begin{pmatrix}\cos\theta_0/\alpha & -\sin\theta_0/\beta\\ -\sin\theta_0/\alpha & -\cos\theta_0/\beta\end{pmatrix}. \tag{4.13}$$

Equation (4.10) is equivalent to Eq. (4.4) with

$$N^{s,\mathrm{inc}}(\mathbf{x},\omega)=\frac{\mu^2b^2}{M\omega^2}\begin{pmatrix}K_1(\mathbf{x},\omega)\left.\dfrac{\partial}{\partial x_2}\right|_{\mathbf{x}=\mathbf{0}} & K_1(\mathbf{x},\omega)\left.\dfrac{\partial}{\partial x_1}\right|_{\mathbf{x}=\mathbf{0}}\\ K_2(\mathbf{x},\omega)\left.\dfrac{\partial}{\partial x_2}\right|_{\mathbf{x}=\mathbf{0}} & K_2(\mathbf{x},\omega)\left.\dfrac{\partial}{\partial x_1}\right|_{\mathbf{x}=\mathbf{0}}\end{pmatrix}, \tag{4.14}$$

where K_m is defined in Eq. (4.5). In the next step, we use now that the differential operators

$$\left.\frac{\partial}{\partial x_i}\right|_{\mathbf{x}=\mathbf{0}}$$

in the product of matrices $N^{s,\mathrm{inc}}(\mathbf{x},\omega)N^{\mathrm{inc}}$ act on the potentials $\varphi^{\mathrm{inc}}(\mathbf{x},\omega)$ and $\psi^{\mathrm{inc}}(\mathbf{x},\omega)$. It is sufficient to use

$$\begin{aligned}\frac{\partial}{\partial x_i}\varphi^{\mathrm{inc}}(\mathbf{x},\omega)|_{\mathbf{x}=\mathbf{0}}&=\frac{i\Omega}{\alpha}(\cos\theta_0;-\sin\theta_0)\varphi^{\mathrm{inc}}(\mathbf{0},\omega),\\ \frac{\partial}{\partial x_i}\psi^{\mathrm{inc}}(\mathbf{x},\omega)|_{\mathbf{x}=\mathbf{0}}&=\frac{i\Omega}{\beta}(\cos\theta_0;-\sin\theta_0)\psi^{\mathrm{inc}}(\mathbf{0},\omega)\end{aligned} \tag{4.15}$$

to write the set of Eqs. (4.10) and (4.11) as

$$\begin{pmatrix}v_1^s(\mathbf{x},\omega)\\ v_2^s(\mathbf{x},\omega)\end{pmatrix}=M^{s,\mathrm{inc}}(\mathbf{x},\omega)\begin{pmatrix}\varphi^{\mathrm{inc}}(\mathbf{0},\omega)\\ \psi^{\mathrm{inc}}(\mathbf{0},\omega)\end{pmatrix} \tag{4.16}$$

and we find

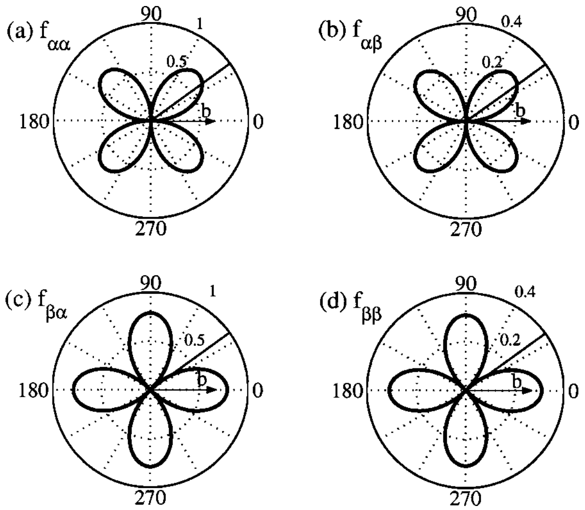

FIG. 5. Scattering function vs θ for an angle between the Burgers vector (along the horizontal axis) and the incident wave direction $\theta_0=\pi/5$ (the direction of the incident wave is indicated in plain line).

$$M^{s,\mathrm{inc}}(\mathbf{x},\omega)=\frac{\mu^2b^2\Omega^2}{M\omega^2}\begin{pmatrix}\frac{K_1(\mathbf{x},\omega)}{\alpha^2}\sin 2\theta_0 & \frac{K_1(\mathbf{x},\omega)}{\beta^2}\cos 2\theta_0\\ \frac{K_2(\mathbf{x},\omega)}{\alpha^2}\sin 2\theta_0 & \frac{K_2(\mathbf{x},\omega)}{\beta^2}\cos 2\theta_0\end{pmatrix}. \tag{4.17}$$

Finally, with $\varphi^{\mathrm{inc}}(\mathbf{0},\omega)$, $\psi^{\mathrm{inc}}(\mathbf{0},\omega)\propto\delta(\omega-\Omega)$, we have

$$\begin{pmatrix}\varphi^s(\mathbf{x},t)\\ \psi^s(\mathbf{x},t)\end{pmatrix}=N^sM^{s,\mathrm{inc}}(\mathbf{x},\Omega)\begin{pmatrix}\varphi^{\mathrm{inc}}(\mathbf{0},t)\\ \psi^{\mathrm{inc}}(\mathbf{0},t)\end{pmatrix}. \tag{4.18}$$

Far from the dislocation, the asymptotic values of K_m are calculated (see the Appendix) and the scattering functions are found by identification between Eqs. (4.8) and (4.18),

$$\begin{aligned}
f_{\alpha\alpha}(\theta)&=\frac{\mu b^2}{2M}\,\frac{e^{i\pi/4}}{\sqrt{2\pi\Omega\alpha^3}}\left(\frac{\beta}{\alpha}\right)^2\sin 2\theta_0\sin(2\theta-2\theta_0),\\
f_{\alpha\beta}(\theta)&=\frac{\mu b^2}{2M}\,\frac{e^{i\pi/4}}{\sqrt{2\pi\Omega\alpha^3}}\cos 2\theta_0\sin(2\theta-2\theta_0),\\
f_{\beta\alpha}(\theta)&=-\frac{\mu b^2}{2M}\,\frac{e^{i\pi/4}}{\sqrt{2\pi\Omega\beta^3}}\left(\frac{\beta}{\alpha}\right)^2\sin 2\theta_0\cos(2\theta-2\theta_0),\\
f_{\beta\beta}(\theta)&=-\frac{\mu b^2}{2M}\,\frac{e^{i\pi/4}}{\sqrt{2\pi\Omega\beta^3}}\cos 2\theta_0\cos(2\theta-2\theta_0),
\end{aligned} \tag{4.19}$$

whose shapes are given in Fig. 5. From Fig. 5 and related formulas (4.19), important features of the elastic wave scattering can be seen: (i) no interaction occurs between the incident wave and the dislocation in the case of an incident longitudinal α wave propagating in a direction parallel or perpendicular to the Burgers vector ($\theta_0=0,\pi/2$); similarly no interaction occurs in the case of an incident shear β wave propagating in directions with angle $\pi/4$ with the Burgers vector. (ii) The scattered longitudinal wave is always zero in the direction of the Burgers vector ($\theta=\theta_0$) and in the direction orthogonal to the Burgers vector while the shear wave reaches its maximum in these directions. Similarly, the shear scattered wave vanishes in directions with angle $\pi/4$ with the Burgers vector (directions where the longitudinal wave reaches its maximum).

However, in a general case, there is no particular behavior of the cross-coupled scattered waves in the incident direction, contrary to the case of scattering by an inhomogeneity studied in Ref. 41, where the cross-coupled scattered waves remain always apart from the incident direction. An important consequence is that there is no simple argument to neglect mode conversion in a pure forward scattering problem.

B. The optical theorem with polarized waves

The cross sections are defined as in the scalar case. Here, the term $\Sigma\mathbf{v}^*\,\mathbf{dS}$ reduces to

$$xd\theta\rho\left(\alpha^2\frac{\partial u_r}{\partial x}v_r^*+\beta^2\frac{\partial u_\theta}{\partial x}v_\theta^*\right).$$

It is easy to find that $\tilde{\sigma}^s$ and $\tilde{\sigma}^t$, normalized with the energy flux $\sigma_0=\rho\Omega^2/2(A_\alpha^2/\alpha+A_\beta^2/\beta)$ of the incident plane wave across a unit surface, verify

$$\frac{d\tilde{\sigma}^s}{d\theta}=\frac{1}{\frac{A_\alpha^2}{\alpha}+\frac{A_\beta^2}{\beta}}\left(\frac{|f_{\alpha\alpha}(\theta)A_\alpha+f_{\alpha\beta}(\theta)A_\beta|^2}{\alpha}+\frac{|f_{\beta\alpha}(\theta)A_\alpha+f_{\beta\beta}(\theta)A_\beta|^2}{\beta}\right), \tag{4.20}$$

$$\begin{aligned}\tilde{\sigma}^t=\frac{1}{\frac{A_\alpha^2}{\alpha}+\frac{A_\beta^2}{\beta}}\Bigg\{&2\Im\left(\sqrt{\frac{2\pi\alpha}{\Omega}}f_{\alpha\alpha}(0)\frac{A_\alpha^2}{\alpha}e^{-i\pi/4}\right)\\
&+2\Im\left(\sqrt{\frac{2\pi\beta}{\Omega}}f_{\beta\beta}(0)\frac{A_\beta^2}{\beta}e^{-i\pi/4}\right)\\
&+2\Im\left[A_\alpha A_\beta\left(\frac{f_{\alpha\beta}(0)}{\sqrt{\alpha}}+\frac{f_{\beta\alpha}(0)}{\sqrt{\beta}}\right)\sqrt{\frac{2\pi}{\Omega}}e^{-i\pi/4}\right]\Bigg\}.\end{aligned} \tag{4.21}$$

The scattering cross-section $\tilde{\sigma}^s$ is deduced from Eq. (4.20),

$$\tilde{\sigma}^s=\frac{1}{\frac{A_\alpha^2}{\alpha}+\frac{A_\beta^2}{\beta}}\left(\frac{\mu b^2}{2M}\right)^2\frac{1}{2\Omega}\left(1+\frac{\beta^4}{\alpha^4}\right)\times\left(\sin 2\theta_0\frac{A_\alpha}{\alpha^2}+\cos 2\theta_0\frac{A_\beta}{\beta^2}\right)^2. \tag{4.22}$$

This expression is in agreement with Ref. 26 where the calculation was performed in the particular case $A_\alpha=0$, $\theta_0=\pi/2$, with a shear wave incident along the Burgers vector. Note that the scattered and total cross sections cannot be split in longitudinal and shear wave portions, because of the mode conversion. Such coupling has already been observed in the case of scattering of ultrasound by flaws in elastic materials[42] or in the case of the scattering of sound by an elastic inclusion.[43] As in the scalar case, it is found that the scattering strength increases with wavelength (see Sec. V). The second relation (4.21) corresponds to the optical theorem for coupled vector waves.

V. CONCLUDING REMARKS

The scattering by a dislocation investigated in this paper is related to a particular interaction that an elastic wave experiences with a dislocation. In addition to the scattering by the dislocation core, which is negligible at wavelength large compared with core size, the incident wave forces the dislocation to move. This motion involves not only the material close by the dislocation core, but also material at a distance from it comparable to the range of the dislocation deformation field. It is this mechanism that is investigated here. As the dislocation moves with an amplitude proportional to the frequency of the incident wave, it is found that the scattering strength increases with the wavelength (the scattering cross section is proportional to Ω^{-1}).

The limit $\Omega \to 0$, in which the scattering cross section diverges, is outside the framework of the present study. This is mainly because two-dimensional analysis assumes that the typical length in the third direction (here the length of the dislocation line) is large compared to the typical in-plane lengths, which fall off for infinite wavelength. In our calculations, the wavelength thus has an explicit lower limit b and an implicit upper limit that three-dimensional analysis would make appear.

This mechanism, although unusual, has been previously observed for an acoustic wave incident on a fluid vortex;[44] solving Navier–Stokes makes appear a motion of the vortex core due to the incident wave, producing scattering of the acoustic wave.

The vector case of coupled longitudinal and shear waves has been investigated here and it is, to the best of our knowledge, the first time that the complete calculation is reported.

In the recent years, experimental works[38–40] have shown pictures of the wave scattered by an individual dislocation in $LiNbO_3$ thanks to x-ray imaging. Comparison with these experimental results would necessitate extracting from the images quantitative information which is still not available.

Also, a natural extension of the present study would be to describe the modification of the wave propagation in the presence of multiple dislocations.[35] A recent experiment suggests that ultrasounds may be used to determine changes in the attenuation and the acoustic velocity due to dislocations.[45] Another possible experiment in this case would be to measure the modification of the resonant frequencies of a sample of material due to the presence of such scatterers. Work is in progress in that direction.

Finally, one can intend to describe the scattering by the dislocation core, i.e., due to the local microstructure near the dislocation line. As previously said, such scattering has a vanishing strength at long wavelengths (for instance, a discussion on this mechanism can be found in Ref. 22 where the author estimates the scattering cross section of order $b^2\Omega/\beta$). Since long means large compared with the core size b, usual situations are always in the range $\lambda \gg b$. Nevertheless, if interest is in that description, care has to be taken when considering the lattice as a continuum and a better description has to be sought with atomistic modeling, as done for instance numerically in Refs. 46 and 47.

ACKNOWLEDGMENTS

We gratefully acknowledge the support of the framework of a French/Chilean collaboration on "Propagation of wave in continuous disordered media," and FONDAP Grant No. 11980002.

APPENDIX: ASYMPTOTIC BEHAVIOR OF THE GREEN FUNCTIONS FOR THE TWO-DIMENSIONAL NAVIER EQUATION

The asymptotic behavior of the Green functions $G^0(\mathbf{x},\omega)$ for $x\to\infty$ can be calculated starting from $G^0(\mathbf{k},\omega)$. With

$$\rho\frac{\partial^2}{\partial t^2}G^0_{im}(\mathbf{x}-\mathbf{x}',t-t')-c_{ijkl}\frac{\partial^2}{\partial x_j\partial x_k}G^0_{lm}(\mathbf{x}-\mathbf{x}',t-t') = \delta(\mathbf{x}-\mathbf{x}')\,\delta(t-t')\,\delta_{im},$$

we obtain

$$G^0(\mathbf{k},\omega)=\frac{1}{\rho\alpha^2}\frac{1}{\gamma^2(k^2-k_\alpha^2)(k^2-k_\beta^2)} \times\begin{pmatrix} k^2-k_\beta^2+(\gamma^2-1)k_2^2 & -(\gamma^2-1)k_1k_2 \\ -(\gamma^2-1)k_1k_2 & k^2-k_\beta^2+(\gamma^2-1)k_1^2\end{pmatrix}. \quad \text{(A1)}$$

It is now sufficient to take the asymptotic form for large x (dominant terms in $1/\sqrt{x}$) of the $\mathbf{k}$-Fourier transform of $G^0(\mathbf{k},\omega)$. After some calculations, we find

$$G^0_{11}(\mathbf{x},\omega)\simeq\frac{1}{4\rho}\sqrt{\frac{2}{\pi\omega}}e^{i\pi/4} \times\left(\frac{\cos^2\theta}{\alpha^{3/2}}\frac{e^{i\omega x/\alpha}}{\sqrt{x}}+\frac{\sin^2\theta}{\beta^{3/2}}\frac{e^{i\omega x/\beta}}{\sqrt{x}}\right), \quad \text{(A2)}$$

$$G^0_{22}(\mathbf{x},\omega)\simeq\frac{1}{4\rho}\sqrt{\frac{2}{\pi\omega}}e^{i\pi/4} \times\left(\frac{\sin^2\theta}{\alpha^{3/2}}\frac{e^{i\omega x/\alpha}}{\sqrt{x}}+\frac{\cos^2\theta}{\beta^{3/2}}\frac{e^{i\omega x/\beta}}{\sqrt{x}}\right), \quad \text{(A3)}$$

$$G^0_{12}(\mathbf{x},\omega)\simeq\frac{1}{4\rho}\sqrt{\frac{2}{\pi\omega}}e^{i\pi/4}\sin\theta\cos\theta \times\left(\frac{1}{\alpha^{3/2}}\frac{e^{i\omega x/\alpha}}{\sqrt{x}}-\frac{1}{\beta^{3/2}}\frac{e^{i\omega x/\beta}}{\sqrt{x}}\right). \quad \text{(A4)}$$

The asymptotic behaviors of K_1 and K_2 defined in Eq. (4.5) are thus deduced

$$
\begin{aligned}
K_1 &= \frac{\partial}{\partial x_2} G_{11}^0(\mathbf{x},\omega) + \frac{\partial}{\partial x_1} G_{21}^0(\mathbf{x},\omega) \\
&\simeq \frac{i\omega}{4\rho}\sqrt{\frac{2}{\pi\omega}}\, e^{i\pi/4}\left(\sin 2\theta \cos\theta \frac{e^{i\omega x/\alpha}}{\alpha^{5/2}\sqrt{x}} \right. \\
&\qquad \left. -\cos 2\theta \sin\theta \frac{e^{i\omega x/\beta}}{\beta^{5/2}\sqrt{x}} \right), \\
K_2 &= \frac{\partial}{\partial x_2} G_{12}^0(\mathbf{x},\omega) + \frac{\partial}{\partial x_1} G_{22}^0(\mathbf{x},\omega) \\
&\simeq \frac{i\omega}{4\rho}\sqrt{\frac{2}{\pi\omega}}\, e^{i\pi/4}\left(\sin 2\theta \sin\theta \frac{e^{i\omega x/\alpha}}{\alpha^{5/2}\sqrt{x}} \right. \\
&\qquad \left. +\cos 2\theta \cos\theta \frac{e^{i\omega x/\beta}}{\beta^{5/2}\sqrt{x}} \right),
\end{aligned}
\tag{A5}
$$

where we have used $(\partial/\partial x_i)(x_i/x)$ for large x.

[1] C. F. Ying and R. Truell, ‘‘Scattering of a plane longitudinal wave by a spherical obstacle in an isotropically elastic solid,’’ J. Appl. Phys. **27**, 1086–1097 (1956).

[2] N. G. Einspruch and R. Truell, ‘‘Scattering of a plane longitudinal wave by a spherical fluid obstacle in an elastic medium,’’ J. Acoust. Soc. Am. **32**, 214–220 (1960).

[3] Y. H. Pao and C. C. Mow, ‘‘Scattering of plane compressional waves by a spherical obstacle,’’ J. Appl. Phys. **34**, 493–499 (1963).

[4] R. M. White, ‘‘Elastic wave scattering at a cylindrical discontinuity in a solid,’’ J. Acoust. Soc. Am. **30**, 771–785 (1958).

[5] T. S. Lewis and D. W. Kraft, ‘‘Mode conversion relation for elastic wave scattered by a cylindrical obstacle in a solid,’’ J. Acoust. Soc. Am. **56**, 1899–1901 (1974).

[6] N. G. Einspruch, E. J. Witterholt, and R. Truell, ‘‘Scattering of a plane transverse wave by a spherical obstacle in an elastic medium,’’ J. Appl. Phys. **31**, 806–818 (1960).

[7] D. W. Kraft and M. C. Franzblau, ‘‘Scattering of elastic waves from a spherical cavity in a solid medium,’’ J. Appl. Phys. **42**, 3019–3024 (1971).

[8] R. J. McBride and D. W. Kraft, ‘‘Scattering of a transverse elastic wave by an elastic sphere in a solid medium,’’ J. Appl. Phys. **43**, 4853–4861 (1972).

[9] S. K. Datta, ‘‘Propagation of SH-waves through a fiber-reinforced composite-elliptic cylindrical fibers,’’ J. Appl. Mech. **42**, 165–170 (1975).

[10] V. K. Varadan, V. V. Varadan, and Y. A. Pao, ‘‘Multiple scattering of elastic waves by cylinders of arbitrary cross section,’’ J. Acoust. Soc. Am. **63**, 1310–1319 (1978).

[11] V. K. Varadan, ‘‘Scattering of elastic waves by randomly distributed and oriented scatterers,’’ J. Acoust. Soc. Am. **65**, 655–657 (1979).

[12] B. Peterson, V. K. Varadan, and V. V. Varadan, ‘‘Scattering of elastic waves by a fluid inclusion,’’ J. Acoust. Soc. Am. **73**, 1487–1493 (1983).

[13] L. W. Schmerr, Jr., *Fundamentals of Ultrasonic Nondestructive Evaluation: A modelling Approach* (Plenum, New York, 1996).

[14] R. K. Ing and M. Fink, ‘‘Time recompression of dispersive Lamb wave using time reversal mirror applications to flaw detection in thin plates,’’ IEEE Ultrasonics Symposium Proceedings, San Antonio, 1996, pp. 659–664.

[15] M. Fink, ‘‘Ultrasound puts material to the test,’’ Phys. World **11**, 41–45 (1998).

[16] J. C. Aldrin and J. D. Achenbach, ‘‘Model and methodology for crack detection on a cylindrical hole containing an elastic insert,’’ AIP Conf. Proc. **615**, 181–188 (2002).

[17] J. D. Achenbach, ‘‘Modeling for quantitative non-destructive evaluation,’’ Ultrasonics **40**, 1–10 (2002).

[18] E. Orowan, ‘‘Zür Kristallplastizität I-III,’’ Z. Phys. **89**, 605–634 (1934).

[19] M. Polanyi, ‘‘Über eine Art Gitterstörung, die einem Kristall plastisch machen könnte,’’ Z. Phys. **89**, 660–664 (1934).

[20] G. I. Taylor, ‘‘The mechanism of plastic deformation of crystals I-II,’’ Proc. R. Soc. London, Ser. A **145**, 362–388 (1934).

[21] J. M. Burgers, ‘‘Some considerations on the fields of stress connected with dislocations in a regular crystal lattice,’’ Proc. K. Ned. Akad. Wet. **42**, 293–378 (1939).

[22] F. R. N. Nabarro, ‘‘The interaction of screw dislocations and sound wave,’’ Proc. R. Soc. London, Ser. A **209**, 278–290 (1951).

[23] J. D. Eshelby, ‘‘Dislocation as a cause of mechanical damping in metals,’’ Proc. R. Soc. London, Ser. A **197**, 396–416 (1949).

[24] J. D. Eshelby, ‘‘The equation of motion of a dislocation,’’ Phys. Rev. **90**, 248–255 (1953).

[25] T. Mura, ‘‘Continuous distribution of moving dislocations,’’ Philos. Mag. **8**, 843–857 (1963).

[26] J. Kiusalaas and T. Mura, ‘‘On the elastic field around an edge dislocation with application to dislocation vibration,’’ Philos. Mag. **9**, 1–7 (1963).

[27] F. Lund, ‘‘Response of a stringlike dislocation loop to an external stress,’’ J. Mater. Res. **3**, 280–297 (1988).

[28] A. V. Granato and K. Lücke, in *Physical Acoustics*, edited by W. P. Mason (Academic, New York, 1966), Vol. 4A.

[29] A. V. Granato and K. Lücke, J. Appl. Phys. **27**, 583 (1956); **27**, 789 (1956).

[30] K. Lücke and A. V. Granato, Phys. Rev. B **24**, 6991 (1981); A. V. Granato and K. Lücke, *ibid.* **24**, 7007 (1981).

[31] G. A. Kneezel and A. V. Granato, Phys. Rev. B **25**, 2851 (1982).

[32] J. S. Koehler, in *Imperfections in Nearly Perfect Crystals*, edited by W. Schockley *et al.* (Wiley, New York, 1952).

[33] A. C. Anderson, in *Dislocations in Solids*, edited by F. R. N. Nabarro (North-Holland, Amsterdam, 1983), Chap. 29.

[34] M. O. Peach and J. S. Koehler, ‘‘The forces exerted on dislocations and the stress fields produced by them,’’ Phys. Rev. **80**, 436–439 (1950).

[35] A. Maurel, J.-F. Mercier, and F. Lund, ‘‘Elastic wave propagation through a random array of dislocations,’’ Phys. Rev. B. (submitted).

[36] J. P. Hirth and J. Lothe, *Theory of Dislocations* (McGraw–Hill, New York, 1982).

[37] F. R. N. Nabarro, *Theory of Crystal Dislocations* (Oxford University Press, Oxford, 1967), as well as reviews by A. M. Kosevich in *Dislocations in Solids*, edited by F. R. N. Nabarro (North-Holland, Amsterdam, 1980), Vol. 1.

[38] E. Zolotoyabko, D. Shilo, and E. Lakin, ‘‘X-ray imaging of acoustic wave interaction with dislocations,’’ Mater. Sci. Eng., A **309**, 23–27 (2001).

[39] D. Shilo and E. Zolotoyabko, ‘‘Visualization of acoustic wave scattering by dislocations,’’ Ultrasonics **40**, 921–925 (2002).

[40] D. Shilo and E. Zolotoyabko, ‘‘Stroboscopic x-ray imaging of vibrating dislocations excited by 0.58 GHz phonons,’’ Phys. Rev. Lett. **91**, 115506/1–4 (2003).

[41] R.-S. Wu, ‘‘The perturbation method in elastic wave scattering,’’ Pure Appl. Geophys. **131**, 605–637 (1989).

[42] J. E. Gubernatis, E. Domany, and J. A. Krumhansl, ‘‘Formal aspects of the theory of the scattering of ultrasound by flows in elastic materials,’’ J. Appl. Phys. **48**, 2804–2811 (1977).

[43] V. A. Korneev and L. R. Johnson, ‘‘Fluctuations of elastic waves due to random scattering from inclusions,’’ J. Comput. Acoust. **9**, 973–991 (2001).

[44] F. Lund and C. Rojas, ‘‘Ultrasound as a probe of turbulence,’’ Physica D **37**, 508–514 (1989).

[45] S. Kenderian, T. P. Berndt, R. E. Green, and B. B. Djordjevic, ‘‘Ultrasonic monitoring of dislocations during fatigue of pearlitic rail steel,’’ Mater. Sci. Eng., A **338**, 90–99 (2003).

[46] H. Koizumi and H. O. K. Kirchner, ‘‘Lattice wave emission from a moving dislocation,’’ Phys. Rev. B **65**, 214104 (2002).

[47] P. Gumbsh and H. Gao, ‘‘Dislocations faster than the speed of sound,’’ Science **283**, 965–968 (1999).